Location of Chlorophyll$_Z$ in Photosystem II†

Dionysios Koulougliotis, Jennifer B. Innes,‡ and Gary W. Brudvig*

Department of Chemistry, Yale University, 225 Prospect Street, New Haven, Connecticut 06511

Received May 5, 1994; Revised Manuscript Received June 28, 1994®

ABSTRACT: Saturation–recovery and progressive microwave power saturation EPR spectroscopies have been used to probe the location of the chlorophyll$_Z^+$ (Chl_Z^+) radical species in Mn-depleted photosystem II (PSII). The spin–lattice relaxation transients of Chl_Z^+ were non-single-exponential due to a dipole–dipole interaction with one of the other paramagnetic centers in PSII. Measurements on CN^--treated, Mn-depleted PSII membrane samples, in which the non-heme Fe(II) is converted into its low-spin, diamagnetic form, confirmed that the non-heme Fe(II) caused the dipolar relaxation enhancement of Chl_Z^+. The saturation–recovery EPR data were fit to a dipolar model [Hirsh, D. J., Beck, W. F., Innes, J. B., & Brudvig, G. W. (1992) *Biochemistry 31*, 532] which takes into account the isotropic (scalar) and orientation-dependent (dipolar) contributions to the spin–lattice relaxation of the radical. The temperature dependence of the dipolar rate constants of Chl_Z^+ was identical to the temperature dependencies recently observed for the stable tyrosine radical, $Y_D^\bullet$, and the special pair bacteriochlorophyll radical, $(BChla)_2^+$, in PSII and in reaction centers from *Rhodobacter sphaeroides*, respectively. Because the non-heme Fe(II) is known to cause a dipolar relaxation enhancement of the radicals in both of the latter cases, this result provides further evidence that the non-heme Fe(II) causes the dipolar relaxation enhancement of Chl_Z^+ and, moreover, demonstrates that the magnetic properties of the non-heme Fe(II) in PSII and in reaction centers from *Rhodobacter sphaeroides* are very similar. By using the known Fe(II)–$(BChla)_2^+$ distance for calibration, we estimate the Fe(II)–Chl_Z^+ distance to be 39.5 ± 2.5 Å. The theory of dipolar relaxation enhancement of a free radical caused by exogenous Dy^{3+} complexes [Innes, J. B., & Brudvig, G. W. (1989) *Biochemistry 28*, 1116] has also been applied to determine the location of Chl_Z^+ relative to the PSII protein surfaces. Chl_Z^+ was found to be located at approximately equal distances from both the luminal and stromal protein surfaces in extrinsic polypeptide-depleted PSII membranes. These results provide the first direct evidence against the assignment of Chl_Z to a Chl monomer analogous to the "voyeur" BChl in the bacterial reaction center and point to histidines-118 in the D1 and D2 proteins as potential ligands of Chl_Z.

Photosystem II (PSII) is a multicomponent membrane-spanning complex of proteins and chromophores which utilizes light energy to initiate electron-transfer reactions and oxidize water to dioxygen. Its oxidized primary electron donor, $P680^+$ [a special chlorophyll (Chl)], is the most powerful oxidant in photosynthesis, having a reduction potential high enough to oxidize its own antenna chlorophyll [E_m is estimated to be ~1.12 V (Klimov et al., 1980)].

The major electron-donation pathway in PSII is from a tetranuclear Mn cluster through a tyrosine residue known as Y_Z (Tyr-161 of the D1 polypeptide) to $P680^+$, and it involves the catalyzed oxidation of H_2O to dioxygen. In addition to this path, there exist at least two alternative electron donors to $P680^+$: cytochrome b_{559} (cyt b_{559}) and a redox-active tyrosine, Y_D (Tyr-160 of the D2 polypeptide). Recent studies have elucidated the mechanisms of these two alternative electron-donation pathways in PSII (Buser et al., 1990, 1992; Buser, 1993).

EPR spectroscopy has been used (Thompson & Brudvig, 1988) to show that photooxidation of cyt b_{559} proceeds via photooxidation of a chlorophyll (known as Chl_Z) in a sequential pathway of electron transfer:

$$\text{cyt } b_{559} \rightarrow Chl_Z \rightarrow P680^+$$

In the same report, it was proposed that photooxidation of Chl_Z is the first step in the process of photoinactivation of the PSII reaction center.

In order to trap Chl_Z in its oxidized form, it is necessary to have cyt b_{559} oxidized prior to illumination, thereby making it unable to rereduce Chl_Z^+. This can be achieved either by chemical oxidation of cyt b_{559} in the dark (de Paula et al., 1985) or by depletion of the 17- and 23-kDa extrinsic polypeptides which causes cyt b_{559} to be converted into its low-potential form and become oxidized during the course of dark adaptation (de Paula et al., 1986). Following illumination at 77 K in either set of samples, a ~10 G wide free radical EPR signal was observed (de Paula et al., 1985, 1986), centered at $g = 2.0024 \pm 0.0003$, which accounted for 80–90% of the reaction center concentration. A similar EPR signal has also been observed in $K_3Fe(CN)_6$-treated thylakoid membranes (Visser & Rijgersberg, 1975) and tentatively assigned to a chlorophyll cation radical. The same signal has alternatively been assigned to a carotenoid cation radical (Nugent et al., 1982), but there are two pieces of evidence arguing against this assignment: (i) the g-value and line width seem to be more consistent with those of a chlorophyll cation radical [compare Okamura et al. (1982) and references cited therein with Grant et al. (1988)]; and (ii) the visible difference spectrum produced under conditions where photooxidation of both the Mn cluster and cyt b_{559} was blocked (Visser et al., 1977) resembled that of a chlorophyll species, and, due to the irreversibility of the light-induced absorbance changes, it was assigned to a chlorophyll molecule other than P680. An EPR signal similar to that of Chl_Z^+ has also been observed in D1/D2/cyt b_{559} preparations (Nugent et al., 1989), establishing the Chl_Z moiety as a cofactor closely associated with the PSII reaction center.

† This work was supported by the National Institutes of Health (GM 32715 and GM 36442).

‡ Present address: Department of Chemistry, Trinity College, Hartford, CT 06106.

® Abstract published in *Advance ACS Abstracts*, September 1, 1994.

0006-2960/94/0433-11814$04.50/0

On the basis of the analogy between the reaction centers of PSII and of the photosynthetic bacterium *Rhodopseudomonas viridis* (Michel & Deisenhofer, 1988), it has been suggested that there are two monomer Chl molecules in PSII adjacent to P680. This is also supported by the presence of five to six Chls in the D1/D2/cyt b_{559} preparations (Nanba & Satoh, 1987; Gounaris et al., 1990; Kobayashi et al., 1990; Montoya et al., 1991). If the PSII reaction center contains these monomer Chls, they may be quite susceptible to oxidation by $P680^+$. Along these lines, it has been hypothesized that Chl_Z is analogous to one of the "voyeur" monomer BChl molecules in the bacterial reaction center and is in close contact with P680 (Thompson & Brudvig, 1988). In this report, we present evidence testing this hypothesis. We have used the pulsed EPR method of saturation–recovery (Hyde, 1979) as well as the continuous-wave (cw) EPR technique of progressive microwave power saturation in order to probe the location of the Chl_Z species in the PSII reaction center.

Saturation–recovery EPR has already been used by our group in order to probe long-range pairwise spin–spin interactions in proteins (Beck et al., 1990, 1991; Hirsh et al., 1992a,b; Koulougliotis et al., 1992; Hirsh & Brudvig, 1993). The non-single-exponential behavior of the spin–lattice relaxation of the observed paramagnet has been attributed to dipole–dipole interactions with another paramagnetic species acting as a relaxation enhancer, a proposal also made by Evelo and Hoff (1991). A dipolar model has been developed (Hirsh et al., 1992a) to fit the observed saturation–recovery traces and extract isotropic (scalar) and orientation-dependent (dipolar) rate constants.

The spin–lattice relaxation of the oxidized Chl_Z^+ radical has been studied in Mn-depleted PSII membranes. In these samples, the non-heme Fe(II) of the electron acceptor side was the only paramagnet able to act as a relaxation enhancer. The analysis of the observed non-single-exponential spin–lattice relaxation of Chl_Z^+ has allowed us to extract the distance between Chl_Z^+ and the non-heme Fe(II) and, in addition, to obtain information on the processes governing the intrinsic relaxation of the radical.

The theory of relaxation enhancement caused by dipolar interactions with rare earth ions (Bloembergen, 1949; Abragam, 1955) as extended by Hyde and Rao (1978) has been recently applied to examine the accessibility of the stable tyrosine radical in PSII, $Y_D^\bullet$, to Dy^{3+} complexes added to the solution (Innes & Brudvig, 1989). By using the same analysis and experimental strategy, we have also estimated the location of Chl_Z relative to the inner and outer protein surfaces of PSII membranes depleted of the extrinsic 17-, 23-, and 33-kDa polypeptides.

MATERIALS AND METHODS

Sample Preparation. PSII membranes were isolated from market spinach leaves by a modified version (Beck et al., 1985) of the isolation procedure described by Berthold et al. (1981). NH_2OH treatment was used in order to deplete PSII of manganese following the method described in Hirsh et al. (1992a). Residual Mn content in these samples was approximately 5%. For saturation–recovery EPR measurements, the concentration of PSII membranes was between 10 and 12 mg of Chl/mL. The samples were extensively dark-adapted on ice for a period of approximately 12 h before being frozen at 77 K in order to reduce the largest possible amount of $Y_D^\bullet$. Less than 15% of Y_D remains oxidized after a >3-h dark adaptation period (Buser et al., 1990). Photooxidation of Chl_Z was achieved by illumination (700 W/m^2) at 77 K for ~20 min. The CN^- derivative of PSII was prepared as follows [according to Sanakis et al. (1994)]: Mn-depleted PSII membranes were resuspended in pH 8.0 resuspension buffer (20 mM Tricine, 15 mM NaCl, 5 mM $CaCl_2$, and 0.4 M sucrose) and dark-adapted overnight in ice water. Following this dark adaptation, an aliquot of a stock NaCN solution (prepared and adjusted to pH 8.0 just prior to use) was added to the PSII membrane sample to give a final NaCN concentration of 360 mM. The CN^--treated, Mn-depleted PSII membrane sample was then dark-adapted for an extra 4 h prior to being frozen at 77 K in complete darkness. Chemical reduction of the CN^--treated samples was performed by adding 50 mM sodium dithionite from a degassed stock solution prepared and adjusted to pH 8.0 just prior to use. For progressive microwave power saturation studies, Tris-washing of the PSII membranes was done following the procedure described in Innes and Brudvig (1989). Ascorbate treatment (5 mM while stirring in the dark on ice for 30 min) was used to reduce $Y_D^\bullet$ in the Tris-washed samples.

Sperm whale myoglobin (Sigma) was prepared in the NO-ligated form (MbNO) as in Innes and Brudvig (1989). Purified *Rhodobactor sphaeroides* reaction centers were kindly provided by Dr. Harry Frank and Shariar Taremi (University of Connecticut, Storrs), and EPR samples were prepared at pH 7.5 in 30% (v/v) ethylene glycol followed by dilution to give a final optical density of 1.1 at 800 nm.

Lanthanide-containing buffers for either PSII (pH 6.0), MbNO (pH 7.0), or *Rb. sphaeroides* reaction centers (pH 7.5) were prepared by chelating $DyCl_3 \cdot 6H_2O$ with an excess (4:5) of EDTA in the corresponding sample buffer. Samples were then resuspended in the Dy^{3+}-containing buffers to give the desired Dy^{3+}–EDTA concentration.

Instrumentation. The progressive microwave power saturation experiments were performed on a Varian E-9 EPR spectrometer. All data presented here were obtained by using a 10-kHz field modulation at 22 K. The signal intensities were measured as follows. For the $(BChla)_2^+$ radical in *Rb. sphaeroides* reaction centers and the Chl_Z^+ radical in PSII, the peak-to-peak height was used. For the $Y_D^\bullet$ tyrosine radical in PSII, the low-field peak-to-base-line height was used. Finally, for MbNO, which exists in two forms in frozen samples (Yonetani et al., 1972), the signal intensities both at the $g \approx 2$ peak and at the low-field shoulder ($g \approx 2.1$) were measured and showed the same concentration dependence for the effect of added Dy^{3+}–EDTA complexes on the microwave power saturation behavior. Temperature control was achieved with an Oxford ESR 900 liquid helium cryostat and calibrated by using a Si-diode sensor at the sample position. A Cr^{3+}/MgO crystal, which remained at room temperature, was inserted via a port in a modified front plate for a Varian E-231 cavity and was used as a microwave power standard on each scan.

Saturation–recovery EPR experiments and continuous-wave (cw) EPR spectroscopy of the oxidized Chl_Z^+ radical in NH_2OH-treated PSII membranes were performed on a home-built X-band pulsed EPR spectrometer (Beck et al., 1991). The magnetic field position was set at the zero-crossing point of the first-derivative spectrum of Chl_Z^+ (see Figure 3), i.e., at the maximum of the corresponding absorption signal. At any given temperature (controlled and calibrated as in the Varian E-9 instrument), three to four saturation–recovery EPR transients were recorded at different levels of observing microwave power in order to determine $1/T_1$ or $k_{1scalar}$ by linear extrapolation to zero power (Beck et al., 1991). A nonlinear regression program written by Dr. Donald Hirsh,

employing the Marquardt algorithm (Press et al., 1989), was used to obtain fits to the saturation–recovery EPR traces.

Spin quantitations of the Q_A^- and Chl_Z^+ free radical species were done by using the EPR signal of the $Y_D^\bullet$ radical as a spin standard. The maximum yield of $Y_D^\bullet$ was obtained by illumination at 0 °C for 8 min, followed by dark-adaptation for 3 min before freezing at 77 K in complete darkness.

THEORY

Saturation–Recovery EPR. In order to explain the spin–lattice relaxation behavior of Chl_Z^+, we used the dipolar model developed recently (Hirsh et al., 1992a). The model was based on the theory of enhancement of the spin–lattice relaxation of a paramagnetic species due to dipolar interactions with neighboring paramagnets developed by Bloembergen (1949) and Abragam (1955, 1961). By assuming that there exist only pairwise interactions between a "slow"- and a "fast"-relaxing paramagnet, we can describe the spin–lattice relaxation rates of the observed ("slow") spin in terms of three pathways: (i) the intrinsic relaxation rate, k_{1i}, defined as the relaxation rate of the observed spin in the absence of the "fast"-relaxing paramagnet; (ii) the relaxation arising from exchange coupling, k_{1ex}, due to spatial orbital overlap between the wavefunctions of the "slow"- and "fast"-relaxing spins; and (iii) the relaxation arising from the dipolar interaction between the two paramagnets, $k_{1\theta}$.

The first two contributions to the relaxation are isotropic and can be represented as a sum, $k_{1scalar}$, where $k_{1scalar} = k_{1i} + k_{1ex}$. The third contribution depends on the angle, θ, between the interspin vector and the external applied magnetic field. The equations outlined by Kulikov and Likhtenstein (1977) and by Goodman and Leigh (1985) to express the angular dependence of the dipolar rate constant ($k_{1\theta}$), as well as the limits and simplifications which apply in our case, have been presented in detail in Hirsh et al. (1992a) and Hirsh and Brudvig (1993). It has been concluded that $k_{1\theta}$ can be simplified for relaxation enhancement by the non-heme Fe(II) by only keeping the "*C*" term of the dipolar alphabet, as

$$k_{1\theta} = k_{1_d}^C \sin^2\theta\cdot\cos^2\theta \qquad (1)$$

where

$$k_{1_d}^C = \frac{3\gamma_s^2\mu_f^2}{r^6}\frac{1}{\omega_s^2 T_{1f}} \qquad (2)$$

In eq 2, r is the interspin distance, γ_s and ω_s are the magnetogyric ratio and the Larmor frequency of the slow-relaxing spin, respectively, and μ_f and T_{1f} are the magnetic moment and the spin–lattice relaxation time of the fast-relaxing spin, respectively.

If a dipolar interaction affects the relaxation of the observed spin, then a separate relaxation rate constant will apply for every possible orientation, θ, and an angular distribution of rates will be produced. Experimentally, one observes all these rates simultaneously superimposed on the saturation–recovery EPR transient which, consequently, exhibits non-single-exponential behavior. It has been shown that the non-single-exponential spin–lattice relaxation behavior for $Y_D^\bullet$ in Mn-depleted PSII (Hirsh et al., 1992a) and for $(BChla)_2^+$ in the reaction center of *Rb. sphaeroides* (Hirsh & Brudvig, 1993) is due to a dipolar interaction with the non-heme Fe(II).

For a nonoriented protein in a frozen solution, the orientation of the interspin vector and the applied magnetic field is random, and the angle, θ, between them can take all possible values between 0 and π. In this case, the saturation–recovery EPR transient can be fit by using the equation:

$$I(t) = 1 - N\int_0^\pi \sin\theta\cdot[e^{-(k_{1scalar}+k_{1\theta})t}]\,d\theta \qquad (3)$$

where $k_{1scalar} = k_{1i} + k_{1ex}$ and $k_{1\theta}$ is expressed by eqs 1 and 2. $I(t)$ is the intensity of the saturation–recovery EPR transient at time t, and N is an adjustable scaling factor. By fitting eq 3 to a saturation–recovery EPR trasient, three parameters are obtained: N, $k_{1scalar}$, and $k_{1\theta}$.

The value of $k_{1scalar}$ will reflect the intrinsic spin–lattice relaxation rate plus any spin–lattice relaxation enhancement due to an exchange interaction between the fast- and slow-relaxing spins. Owing to the large separation of the spins in Mn-depleted PSII, a significant contribution to the spin–lattice relaxation rate of Chl_Z^+ from an exchange interaction is not expected. Indeed, the value of $k_{1scalar}$ was found to be equal to the intrinsic spin–lattice relaxation rate for $Y_D^\bullet$ in Mn-depleted PSII (Hirsh et al., 1992a) and for $(BChla)_2^+$ in the reaction center of *Rb. sphaeroides* (Hirsh & Brudvig, 1993).

The value of $k_{1\theta}$ will reflect the dipolar interaction between the two spins, as shown in eqs 1 and 2. The dipolar rate constant, $k_{1_d}^C$, has two terms which are temperature dependent, μ_f and T_{1f}, and they are associated with the fast-relaxing spin. In this way, the temperature dependence of $k_{1_d}^C$ provides a signature for the fast relaxer. If the assumption of pairwise spin–spin interactions can be shown to be valid, then the observation of an identical temperature dependence of $k_{1_d}^C$ for different observed spins is direct evidence that, in all cases, the fast-relaxing spin is the same. A $\sim T^{1.65}$ temperature dependence of $k_{1_d}^C$ is the signature for the non-heme Fe(II) acting as the spin–lattice relaxation enhancer of $Y_D^\bullet$ in Mn-depleted PSII (Hirsh et al., 1992a) and of $(BChla)_2^+$ in the reaction center of *Rb. sphaeroides* (Hirsh & Brudvig, 1993). In addition, the relative magnitudes of the observed $k_{1_d}^C$'s will reflect the proximity of the fast-relaxing spin to the observed spin. Taking into account that the $(BChla)_2^+$–Fe(II) distance is known to be equal to 28 Å from the solved crystal structure (Yeates et al., 1987), one can estimate the unknown distance between the non-heme Fe(II) and Chl_Z^+ from the relative magnitudes of $k_{1_d}^C$ measured for $(BChla)_2^+$ and Chl_Z^+ in the reaction center of *Rb. sphaeroides* and Mn-depleted PSII, respectively (eq 4).

$$\frac{r_{Chl_Z^+-Fe(II)}}{r_{(BChla)_2^+-Fe(II)}} = \sqrt[6]{\frac{k_{1_d}^C[(BChla)_2^+]}{k_{1_d}^C(Chl_Z^+)}} \qquad (4)$$

Progressive Microwave Power Saturation. The accessibility of Chl_Z^+ to the aqueous phase was studied by measuring the changes of the quantity $P_{1/2}$ (microwave power at half-saturation) upon addition of various concentrations of Dy^{3+}–EDTA complexes to the solution. $P_{1/2}$ is proportional to $(H_{1/2})^2$, the microwave field needed to saturate a spin packet, and defined by $(H_{1/2})^2 = 1/\gamma^2 T_1 T_2$ (Portis, 1953; Castner, 1959; Beinert & Orme-Johnson, 1967). The empirical equation used to fit the EPR derivative signal amplitude (S) is

$$S = \frac{k\sqrt{P}}{(1 + P/P_{1/2})^{b/2}} \qquad (5)$$

where b is the inhomogeneity parameter varying between b

= 1 (completely inhomogeneous line broadening) and b = 3 (completely homogeneous line broadening), k is a proportionality factor, and P is the microwave power applied. The determination of $P_{1/2}$ values was done as described in Innes and Brudvig (1989).

The exogenous Dy^{3+} complex will enhance the relaxation of the Chl_Z^+ radical through dipole–dipole interactions. In this way, the $P_{1/2}$ value of Chl_Z^+ will be increased, and since relaxation mechanisms are additive, one can formulate the equation:

$$(P_{1/2})_{\text{measured}} = (P_{1/2})_{\text{intrinsic}} + (P_{1/2})_{\text{Dy-induced}} \quad (6)$$

In this case, a single free radical imbedded in the protein "feels" the interactions of multiple Dy^{3+}–EDTA species. This dictates a summation over all the Dy^{3+}-induced relaxation contributions. Innes and Brudvig (1989) have presented the theory used to treat this problem, tested it successfully in two model systems (MbNO and *Rb. sphaeroides* reaction centers), and used it to determine the distances of $Y_D^\bullet$ from both (inner and outer) protein surfaces in PSII membranes. They developed the theoretical expressions of Hyde and Rao (1978) to deduce the equation describing the Dy^{3+} effect in the relaxation of the observed spin:

$$\Delta P_{1/2} = C \cdot \Delta[Dy^{3+}] \cdot \sum_i r^{-6} \quad (7)$$

where $\Delta P_{1/2}$ is the change in $P_{1/2}$ caused by a given change in the concentration of Dy^{3+}, $\Delta[Dy^{3+}]$, C is a constant representing all terms that are expected to remain much the same for all dipolar interactions between free radicals and Dy^{3+} ions, and $\sum_i r^{-6}$ is the sum of distances of the free radical from all possible sites of the Dy^{3+} ion. It was also shown that Dy^{3+}–EDTA is randomly dispersed in solutions of MbNO, *Rb. sphaeroides* reaction centers, and PSII (Innes & Brudvig, 1989). In this case, the value of $\sum_i r^{-6}$ depends on the excluded volume of the protein and the location of the endogenous paramagnetic center in the protein. Analytical expressions for $\sum_i r^{-6}$ were derived from the known structures of MbNO and *Rb. sphaeroides* reaction centers and used to obtain the constant, C, in order to allow distance estimates for systems with an unknown structure. Equivalent results were obtained with both MbNO and *Rb. sphaeroides* reaction centers, demonstrating that the restuls are applicable to both water-soluble and membrane proteins.

In Tris-treated PSII membranes, the extrinsic polypeptides have been depleted, and the Dy^{3+}–EDTA complexes can approach from both protein surfaces. By approximating the PSII membrane sample as a planar sheet, the quantity $\sum_i r^{-6}$ was calculated to be equal to

$$\sum_i r^{-6} = \frac{\pi}{6}(r_1^{-3} + r_2^{-3}) \quad (8)$$

where r_1 and r_2 are the distances of the observed radical (Chl_Z^+) to the outer and inner protein surfaces, respectively. In thylakoid membranes, where the inner surface is sealed from approach of Dy^{3+}–EDTA complexes, the analogous expression was shown to be

$$\sum_i r^{-6} = \frac{\pi}{6} r_1^{-3} \quad (9)$$

RESULTS

Saturation–Recovery EPR. (A) Role of Cytochrome b_{559} and Q_A^-. In order to photooxidize Chl_Z, cyt b_{559} must already be oxidized. In the following experiments, we have not pretreated the samples with K_2IrCl_6, the chemical oxidant of cyt b_{559} used in previous studies (de Paula et al., 1985), in order not to add another paramagnet to the system. Instead, NH_2OH treatment was quite effective in changing cyt b_{559} into its low-potential form which was autooxidized during the long (~12 h) dark adaptation period on ice. The cw dark EPR spectrum (not shown) exhibited a prominent signal at g = 3.0, indicative of oxidized cyt b_{559}. Upon illumination at 77 K, the signal at g = 3.0 was increased by only ~20–25%, indicating that at least 75% of cyt b_{559} was oxidized initially in the dark.

In addition to cyt b_{559} being almost fully oxidized, low-temperature illumination induced a charge separation resulting in the formation of Q_A^-–Fe^{2+} on the electron acceptor side of PSII (evidenced by the appearance of the g = 1.9 EPR signal). Thus, there exist two paramagnets in our system, cyt b_{559}(ox) and Q_A^-, in addition to the non-heme Fe(II), that could act to enhance the spin–lattice relaxation of Chl_Z^+. This fact could invalidate our assumption of pairwise dipolar interactions depending on the potency and proximity of these relaxers. The following experiments were performed to examine this possible complication.

Untreated, extensively dark-adapted PSII membranes, where the Mn cluster is poised in its diamagnetic S_1 resting state (Koulougliotis et al., 1992), were illuminated at 77 K for 15 min in order to oxidize cyt b_{559} and induce Q_A^-–Fe^{2+}. The spin–lattice relaxation behavior of $Y_D^\bullet$ was then examined, and the non-single-exponential saturation–recovery EPR transients were analyzed. The dipolar rate constants extracted from fits to saturation–recovery EPR data taken over the temperature range 4.0 K $\leq T \leq$ 50 K were indistinguishable from those observed in the dark-adapted sample. This shows that neither cyt b_{559}(ox) nor Q_A^- provides a relaxation pathway efficient enough to enhance the relaxation of $Y_D^\bullet$ more than the non-heme Fe(II) already does.

The relaxation behavior of $Y_D^\bullet$ in CN^--treated, Mn-depleted PSII membranes was also examined. In these samples, cyt b_{559} was autoxidized in the dark and the non-heme Fe(II) converted to its low-spin, diamagnetic form. The saturation–recovery EPR transients obtained for $Y_D^\bullet$ were single-exponential and much slower than in Mn-depleted samples that had not been treated with NaCN. These results show that the non-heme Fe(II) is the only effective relaxation enhancer of $Y_D^\bullet$ in Mn-depleted PSII (D. Koulougliotis, X.-S. Tang, B. A. Diner, and G. W. Brudvig manuscript in preparation).

Low-temperature illumination (77 K for 20 min) of CN^--treated, Mn-depleted PSII membranes induces the Chl_Z^+–Q_A^- charge separation. In this case, the exchange interaction between Q_A^- and Fe(II) (responsible for the Q_A^-–Fe^{2+} EPR signal) is lost since the non-heme Fe(II) is diamagnetic. Thus, the light-induced g = 2 EPR signal (Figure 1a, solid line) has contributions from both the Chl_Z^+ and Q_A^- species.

The EPR signal corresponding to Q_A^- can be observed without any interference in CN^--treated, Mn-depleted PSII membranes after treatment with sodium dithionite in the dark. Figure 1a (dotted line) shows the Q_A^- EPR signal induced at its maximum yield (~0.9 spin per PSII reaction center, attained after 6 h of treatment with CN^- plus dithionite). The integrated intensity of the light-induced Chl_Z^+–Q_A^- EPR signal (Figure 1a, solid line) is 2 times larger than the maximal Q_A^- signal, as expected for the superposition of EPR signals from the two radicals.

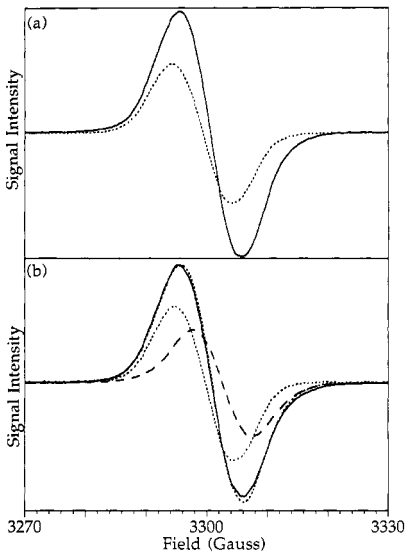

FIGURE 1: (a) cw EPR spectra of the following: (i) CN^--treated, Mn-depleted PSII membranes after illumination at 77 K for ~20 min (solid line); (ii) CN^-- and dithionite-treated, Mn-depleted PSII membranes frozen in the dark (dotted line). (b) cw EPR spectra of the following: (i) CN^--treated, Mn-depleted PSII after illumination at 77 K for ~20 min (solid line) [a different PSII preparation was used from the one for Figure 1a, (ii)]; (ii) CN^-- and dithionite-treated, Mn-depleted PSII membranes frozen in the dark (dotted line, "pure" Q_A^- signal); (iii) Mn-depleted PSII after illumination at 77 K for ~20 min (dashed line, "pure" Chl_Z^+ signal). The intensities of spectra ii and iii have been scaled so that their addition reproduces the intensity and position of spectrum i. Their sum is shown as the dotted line superimposed on spectrum i. The relative integrated intensities of spectra i, ii, and iii are 1.00, 0.56, and 0.44, respectively. Experimental conditions for all spectra were the following: sample concentration, 4 mg of Chl/mL; temperature, 9 K; microwave frequency, 9.07 GHz; field-modulation amplitude, 4.0 G; microwave power, 0.72 μW; field-modulation frequency, 100 kHz.

The EPR signal observed at $g = 2.0$ after low-temperature illumination of an independently prepared CN^--treated, Mn-depleted PSII sample is shown in Figure 1b (solid line). The "pure" Chl_Z^+ ($g = 2.0024$) and Q_A^- ($g = 2.0040$) signals are shown in the same figure with dashed and dotted lines, respectively, and are properly scaled so that their addition reproduces the intensity and position of the combined Chl_Z^+–Q_A^- signal. The reproducible way with which the Chl_Z^+–Q_A^- charge separation can be induced with a relative spin-intensity ratio of approximately 1:1 is an initial indication that a unique chlorophyll molecule is photooxidized.

Figure 2 shows the results of saturation–recovery EPR experiments performed independently on the following signals: (i) the "pure" signal of the Q_A^- free radical species (Figure 1a, dotted line); (ii) the "pure" signal of the Chl_Z^+ free radical species (Figure 1b, dashed line); and (iii) the combined Chl_Z^+–Q_A^- signal (Figure 1a, solid line). The saturation–recovery EPR transients obtained for the "pure" Q_A^- EPR signal were, as expected, well fit by a single exponential; thus, only the intrinsic spin–lattice relaxation contributes to the relaxation of Q_A^- in CN^-- and dithionite-treated, Mn-depleted PSII. These results are shown as a function of temperature with open square symbols. The saturation–recovery transients obtained for the "pure" Chl_Z^+ signal were non-single-exponential and were analyzed by using the dipolar model (vide infra). In Figure 2, the scalar rate constants, $k_{1scalar}$, extracted from the dipolar-model fits are plotted. As explained under Theory, if the analysis according to the dipolar model is valid, then the $k_{1scalar}$ values should represent the intrinsic relaxation rate of the observed radical (i.e., $k_{1scalar} = k_{1intrinsic} = 1/T_1$), provided that the separation between spins is large enough such that k_{1ex} is negligible.

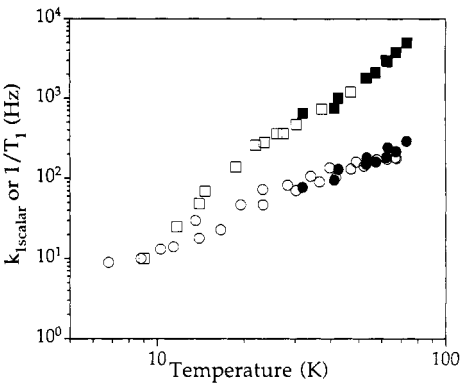

FIGURE 2: Temperature dependence of $1/T_1$ for Q_A^- in CN^-- and dithionite-treated, Mn-depleted PSII membranes (□), $k_{1scalar}$ for Chl_Z^+ induced after 77 K illumination in Mn-depleted PSII membranes (○), and the $1/T_1$ values of the fast (■) and slow (●) components extracted from the double-exponential fits for the combined Chl_Z^+–Q_A^- signal induced after 77 K illumination in CN^--treated, Mn-depleted PSII membranes. In this plot, $1/T_1$ denotes the spin–lattice relaxation rate for a noninteracting spin, and the values were extracted from exponential fits to the data; $k_{1scalar}$ denotes the isotropic contribution to the spin–lattice relaxation rate for an interacting spin, and the values were extracted from fits to the dipolar model (eq 3).

The free radical signal centered at $g \approx 2.0036$, produced after 77 K illumination in CN^--treated, Mn-depleted PSII samples, is due to both the Chl_Z^+ and Q_A^- species. Thus, the saturation–recovery EPR measurement on the combined Chl_Z^+–Q_A^- signal will probe the relaxation of both Q_A^- and Chl_Z^+ simultaneously, and, therefore, the recoveries are not expected to be single-exponential. However, if neither Q_A^- nor Chl_Z^+ experiences a dipolar contribution to their relaxation in the CN^--treated sample, then one would expect the recoveries to be satisfactorily fit by a double exponential. The rate constants obtained from the double-exponential fits are shown in Figure 2 with solid symbols. We observe that the rate constants for the fast component show a temperature dependence and magnitude identical, within experimental error, to those directly measured for the intrinsic relaxation rate constants of Q_A^-. Correspondingly, the rate constants for the slow component show the same temperature dependence and magnitude as the scalar rate constants extracted from the dipolar-model fits when the saturation–recovery EPR experiment is done on the "pure" Chl_Z^+ radical in a non-CN^--treated, Mn-depleted PSII sample (vide infra). The good agreement of the spin–lattice relaxation rates of the fast and slow components extracted from the double-exponential fits with those separately measured for Q_A^- and Chl_Z^+ validates our assumption that the two species relax independently. In addition, these results provide direct evidence that cyt b_{559} (which was oxidized in the course of these measurements) does not affect the relaxation of Chl_Z^+.

(B) Spin–Lattice Relaxation of Chl_Z^+. Figure 3 shows the EPR spectra of extensively dark-adapted NH_2OH-treated PSII membranes in the $g = 2.0$ region before and after illumination at 77 K. The illumination produced a 10 G wide EPR signal corresponding to Chl_Z^+ (used as the "pure" Chl_Z^+ signal in Figure 1), with an integrated signal intensity ~18 times larger (average of three independent measurements) than that from the residual $Y_D^\bullet$ present in the dark-adapted sample. We estimate that the contribution of the $Y_D^\bullet$ radical to the signal after illumination is less than 5%.

A typical saturation–recovery EPR transient of the Chl_Z^+ radical is shown in Figure 4a with the dipolar-model fit superimposed. The residuals for single-exponential and dipolar

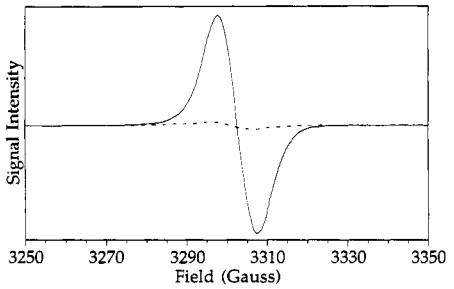

FIGURE 3: cw EPR spectra of long-term dark-adapted, Mn-depleted PSII taken in the dark (dashed line) and after illumination at 77 K for 15 min (solid line). Experimental conditions were the same as in Figure 1.

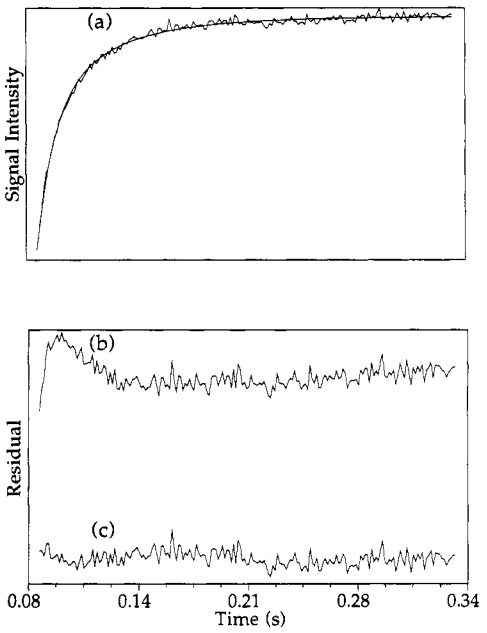

FIGURE 4: (a) Saturation–recovery EPR transient obtained for Chl$_Z^+$ in Mn-depleted PSII at 11.5 K with the fit by using the C term of the dipolar model (eq 3) superimposed. The observing microwave power was 0.36 μW, the saturating microwave pulse power was 72 mW, and the pulse was of 37-ms duration. The residuals (difference between the saturation–recovery EPR transient and the fitted curve) are shown for (b) the single-exponential fit and (c) the dipolar-model fit.

fits show that the transient is non-single-exponential. This behavior held for the entire temperature range, 6 K $\leq T \leq$ 68 K, examined. On the basis of the evidence presented in the previous section and the arguments under Theory, we attribute the non-single-exponential recovery of Chl$_Z^+$ to a dipolar interaction with the non-heme Fe(II).

This assignment is additionally supported from the observed temperature dependence of the dipolar rate constants shown in Figure 5. The temperature dependencies of the dipolar rate constants of $Y_D^\bullet$ in Mn-depleted PSII membranes, of (BChla)$_2^+$ in the reaction center from *Rb. sphaeroides* (Hirsh & Brudvig, 1993), and of Chl$_Z^+$ in Mn-depleted PSII membranes are all equal within experimental error. These results provide further evidence that the non-heme Fe(II) enhances the relaxation of the observed spin in all three cases. By using eq 4 and the values of $k_{1_d}^C$ plotted in Figure 5, we estimate a distance between Chl$_Z^+$ and Fe(II), $r_{Chl_Z^+-Fe(II)}$ = 40 ± 2 Å.

Figure 6 shows the temperature dependence of the scalar rate constants of Chl$_Z^+$, together with $k_{1scalar}^C$ of (BChla)$_2^+$ from the reaction center of *Rb. sphaeroides* and the single-exponential ($1/T_1$) rate constants for two different model

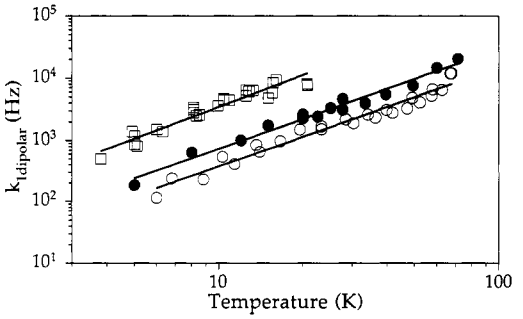

FIGURE 5: Temperature dependence of k_{1d}^C for (BChla)$_2^+$ (□) in chromatophore-bound reaction centers of *Rb. sphaeroides*, $Y_D^\bullet$ (●) in Mn-depleted PSII membranes, and Chl$_Z^+$ (○) in Mn-depleted PSII membranes. The data for (BChla)$_2^+$ and $Y_D^\bullet$ were taken from Hirsh and Brudvig (1993). The best power-law fits ($k_{1d}^C = AT^n$) are shown superimposed for each set of rate constants: (BChla)$_2^+$, $k_{1d}^C = (72 \pm 15)T^{1.7\pm0.1}$; $Y_D^\bullet$, $k_{1d}^C = (20 \pm 5)T^{1.6\pm0.1}$; and Chl$_Z^+$, $k_{1d}^C = (9 \pm 1)T^{1.65\pm0.05}$.

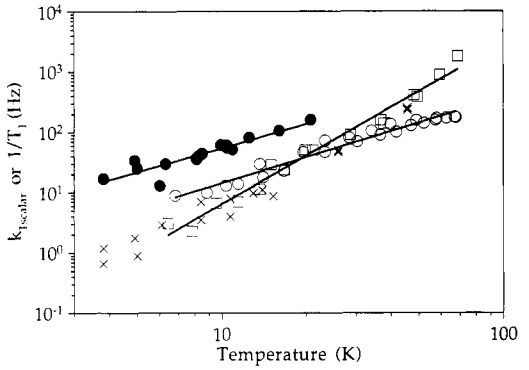

FIGURE 6: Temperature dependence of $1/T_1$ for [Ni(OEP)$^{\bullet/2}$]$_2$ (□) and (BChla)$^+$ (×) and $k_{1scalar}$ for (BChla)$_2^+$ (●) in chromatophore-bound reaction centers of *Rb. sphaeroides* and for Chl$_Z^+$ (○) in Mn-depleted PSII membranes. The data for [Ni(OEP)$^{\bullet/2}$]$_2$, (BChla)$^+$, and (BChla)$_2^+$ were taken from Hirsh and Brudvig (1993). The best power-law fits are shown superimposed: $1/T_1$([Ni(OEP)$^{\bullet/2}$]$_2$) = $0.01T^{2.6\pm0.1}$, $k_{1scalar}$[(BChla)$_2^+$] = $2.5T^{1.3\pm0.1}$, and $k_{1scalar}$(Chl$_Z^+$) = $0.5T^{1.4\pm0.1}$.

systems: a BChla$^+$ monomer and an Ni(II) porphyrin dimer, [Ni(II)(OEP$^{\bullet/2}$)]$_2$. The temperature dependence of $k_{1scalar}^C$ of Chl$_Z^+$ is not similar to the $T^{2.5}$ temperature dependence observed for $1/T_1$ of the two model systems or the $k_{1scalar}^C$ values of $Y_D^\bullet$ and a model UV-irradiated tyrosine radical (Hirsh et al., 1992a). The same unusual temperature dependence ($\sim T^1$) was found for $k_{1scalar}^C$ of (BChla)$_2^+$ in the *Rb. sphaeroides* reaction center, and it is indicative of a one-phonon direct spin–lattice relaxation process. A comparison between $k_{1scalar}^C$[(BChla)$_2^+$] and $k_{1scalar}^C$(Chl$_Z^+$) shows that the latter are consistently ~5-fold smaller.

Progressive Microwave Power Saturation. By changing the concentration of Dy^{3+}–EDTA added to the solution and probing the effect on the $P_{1/2}$ value of the free radicals of interest in MbNO, the reaction center from *Rb. sphaeroides*, and Tris-washed PSII membranes, we have constructed the plots of $\Delta P_{1/2}$ vs $\Delta[Dy^{3+}]$ shown in Figure 7. The slopes of the plots ($m = \Delta P_{1/2}/\Delta[Dy^{3+}]$) are linear within experimental error, indicating that there is no specific binding.

MbNO and *Rb. sphaeroides* reaction centers were used as model systems. By assuming a random distribution of Dy^{3+}–EDTA in solution and the results of Innes and Brudvig (1989), we have calculated $\Sigma_i r^{-6}$ for both model systems. Then, by using eq 7, we determined the constant, C, to be C_{MbNO} = 2.28 × 10^3 mW Å^3/mM and $C_{(BChla)_2^+}$ = 2.26 × 10^3 mW Å^3/mM.

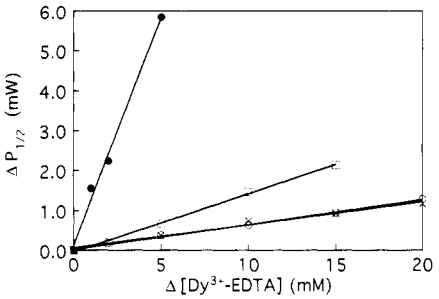

FIGURE 7: Change of the microwave power at half-saturation ($\Delta P_{1/2}$) vs change in the concentration of added Dy^{3+}–EDTA ($\Delta[Dy^{3+}]$) for MbNO (●), $(BChla)_2^+$ in purified reaction centers of *Rb. sphaeroides* (□), $Y_D^\bullet$ in Tris-washed PSII membranes (×), and Chl_Z^+ in Tris-washed PSII membranes (○). All measurements were taken at 22 K with 10-kHz field-modulation frequency. The slopes of the linear fits ($m = \Delta P_{1/2}/\Delta[Dy^{3+}]$) shown for each set of measurements are the following: 1.14 ● 0.06 for MbNO, 0.146 ● 0.004 for $(BChla)_2^+$, 0.063 ± 0.002 for $Y_D^\bullet$, and 0.058 ± 0.004 for Chl_Z^+.

Measurements on $Y_D^\bullet$ of $\Delta P_{1/2}$ vs $\Delta[Dy^{3+}]$ were presented in Innes and Brudvig (1989), but they were performed at different experimental conditions (T = 14 K, 100-kHz field modulation) from the data shown in Figure 7. In this earlier work, it was found that $Y_D^\bullet$ is buried approximately at the middle of the PSII membrane when the extrinsic polypeptides were depleted. Measurements on $Y_D^\bullet$ were also made on thylakoid membranes in which only the outer membrane surface is exposed to Dy^{3+}–EDTA. Thus, it was possible to determine the distances of $Y_D^\bullet$ from both the inner and outer surfaces. However, this was not possible for Chl_Z^+ because Chl_Z^+ cannot be induced in thylakoid membranes without a considerable contribution from $Y_D^\bullet$. Therefore, the distance of Chl_Z^+ from the outer protein surface cannot be determined separately. However, the problem of having two unknowns in eq 8, r_1 and r_2, is circumvented by the following observation. Comparing the slopes, m, in Figure 7 for $Y_D^\bullet$ and Chl_Z^+ in Tris-washed PSII membranes, we observe that they are identical within experimental error; i.e., the Dy^{3+}-induced effect is the same for both radicals. This should happen only if their distances from the Dy^{3+} sites are similar. Since $Y_D^\bullet$ is buried near the center of the PSII protein, the same can be concluded for Chl_Z^+; i.e., $r_1 \approx r_2 = \rho$. Therefore, eq 8 becomes $\sum_i r^{-6} = (\pi/3)\rho^{-3}$, and from eq 7, we get $(\pi/3)\rho^{-3} = m/C$. By using the values of C determined from both model systems, we can determine ρ. The actual distance of Chl_Z^+ to the protein surfaces is obtained by subtracting 6.1 Å from the calculated ρ, corresponding to the radius of the Dy^{3+}–EDTA complex in van der Waals contact with the surface of the protein. After this subtraction, it was found that $r_{Chl_Z\text{-protein surfaces}}$ = 27.1 ± 1 Å by using MbNO and 27.6 ± 1 Å by using *Rb. sphaeroides* reaction centers as model systems, respectively. The distances calculated with the two different models agree to within 1 Å. The uncertainties quoted are based on the errors in the slopes, m, from the linear fits of $\Delta P_{1/2}$ vs $\Delta[Dy^{3+}]$.

DISCUSSION

Location of Chl_Z. In this report, the pulsed EPR technique of saturation–recovery was used to probe the pairwise dipolar interaction between Chl_Z^+ and the non-heme Fe(II) in PSII. Control experiments showed that the relaxation enhancement of Chl_Z^+ provided by the non-heme Fe(II) is much stronger compared to the contributions from cyt b_{559}(ox) and Q_A^- also present in the sample. Further evidence in support of a pairwise interaction between Chl_Z^+ and Fe(II) is provided by the $\sim T^{1.6}$ temperature dependence of the dipolar rate constants. This is identical to the temperature dependencies observed (Hirsh & Brudvig, 1993) for two different free radicals [$Y_D^\bullet$, $(BChla)_2^+$] interacting through a dipolar mechanism with the non-heme Fe(II). In this earlier work, the issue was raised of the term of the dipolar alphabet that has the largest contribution to the relaxation of the observed radical. It was shown that the use of the B term of the dipolar alphabet [where $k_{1d} \propto (1 - 3\cos^2\theta)^2$] resulted in temperature dependencies for the dipolar rate constants that were equal, within error, to the ones obtained by using the C term. The saturation–recovery EPR transients obtained for Chl_Z^+ were also analyzed with the B term, and it was found that $k_{1d}^B = (1.8 \pm 0.4)\text{-}T^{1.65\pm0.05}$. The analogous equation for the $(BChla)_2^+$ radical is $k_{1d}^B = (13 \pm 3)T^{1.8\pm0.1}$ (Hirsh & Brudvig, 1993). If we use the dipolar rate constants extracted from the B term dipolar-model fit and eq 4, we obtain a distance between the non-heme Fe(II) and Chl_Z of 39 ± 3 Å. This value is identical to the one determined from the C term fit within experimental error. By combining both results and the total error, we estimate the distance to be $r_{Chl_Z^+\text{-Fe(II)}}$ = 39.5 ± 2.5 Å.

The analysis presented above was made under the assumption that a unique chlorophyll molecule is photooxidized to produce Chl_Z^+. This fact is supported by the following lines of evidence: (i) All quantitations of the Chl_Z^+ radical EPR signal performed in different sample preparations in the past (de Paula et al., 1985; Buser et al., 1992), and in this work, have shown that it is not possible to induce the signal with a yield higher than 1 spin per PSII reaction center. (ii) The directly measured intrinsic relaxation rates ($1/T_1$) of Chl_Z^+ in CN^--treated, Mn-depleted PSII membranes were shown to be identical with the scalar rate constants extracted for the same species from the dipolar-model fits. This effect is shown in Figure 2 for two different PSII preparations. If a distribution of chlorophyll molecules was photooxidized, then one would not expect their "collective" relaxation rate to be reproducibly the same and also to show the same temperature dependence. (iii) The dipolar rate constants shown for Chl_Z^+ in Figure 5 are from two different Mn-depleted PSII preparations. Their reproducibility also provides strong evidence that a unique chlorophyll molecule was photooxidized. If this were not the case, then one would expect the spin–lattice relaxation rates to differ, modulated by the distance of the oxidized species from the non-heme Fe(II).

In the reaction center of *Rb. sphaeroides*, the distance between the non-heme Fe(II) and each of the two "voyeur" monomer BChl molecules is approximately 25 Å (Yeates et al., 1987). The corresponding distance in the reaction center of *Rps. viridis* is ~27 Å (Deisenhofer et al., 1984; determined from the crystal structure coordinates stored in the Brookhaven database). If the monomer Chls exist also in PSII and the structural analogy with the bacterial system holds, we then conclude that Chl_Z of PSII is not homologous to one of the "voyeur" chlorophylls, since the distance of ~40 Å from Chl_Z to the non-heme Fe(II) is much larger than expected based on the analogy.

The effect of exogenous Dy^{3+}–EDTA complexes on the microwave power saturation behavior of Chl_Z^+ allowed us to determine its distances from the surfaces of the PSII protein. It was concluded that Chl_Z is imbedded near the center of the PSII protein complex at a distance of about 27 Å from both the inner and outer protein surfaces. Thus, an additional constraint is added to the possible positions of Chl_Z. It has to be placed on a plane passing through the center of the PSII protein complex and at the same time 40 Å away from the non-heme Fe(II). By using the structure of the L and M

subunits of the bacterial reaction center of *Rps. viridis* as a reference, we checked where the protein is intersected by a sphere of 40 Å centered at the non-heme Fe. The sphere intersected the L/M structure only at the ends of two to three transmembrane helices close to the cytoplasmic side of the membrane. However, several residues on the lipid-exposed surface of transmembrane helices A and B of the L and M subunits are near the middle of the membrane and are also close to 40 Å from the non-heme Fe(II). This suggests that a residue located near the hydrophobic surface of the D1/D2 structural unit of PSII could provide a ligand to Chl$_Z$, always keeping in mind the assumed analogy with the bacterial reaction center. By checking the sequences of the D1 and D2 polypeptides, it has been noticed (Ruffle et al., 1992) that there exist two conserved histidine residues (D1-His118, D2-His118) which are near the middle of the predicted transmembrane B helices and have not been identified as ligands to any of the cofactors. In this reference, it was suggested that these side chains "are interacting with either another protein or a cofactor, since it is unlikely that a charged residue would be conserved and facing the lipid". The corresponding residues in the *Rps. viridis* reaction center are L-Cys92 and M-Phe119, both of which are located close to the surface of the L/M structural unit. The sulfur atom of Cys92 and the phenyl ring of Phe119 are located at distances of ~36 and ~39 Å from the non-heme Fe(II). These values for the distances are close to the value determined for the Fe(II)–Chl$_Z^+$ distance of 39.5 ± 2.5 Å in PSII. Recently, Schelvis et al. (1994) used transient absorption difference spectroscopy to probe energy transfer and charge separation in the isolated PSII reaction center. Upon selective excitation of the short-wavelength pigments, they measured a 30 ps energy-transfer event from an accessory chlorophyll to P680, which was translated to a 30 Å center-to-center distance by using Förster energy-transfer theory. This distance led them to propose that histidines-118 of the D1 and D2 polypeptides are "likely binding sites of the chlorophylls nearest to the long-wavelength pigments, P680 and pheophytin". Thus, the possibility that either D2-His118 or D1-His118 provides the fifth ligand to Chl$_Z$ seems quite plausible, in accordance with Ruffle et al. (1992), Schelvis et al. (1994), and the results of this work. This proposal could be tested experimentally by site-directed mutagenesis.

Intrinsic Relaxation of Chl$_Z^+$. As shown in Figure 6, the scalar rate constants of Chl$_Z^+$ follow a $T^{1.4}$ temperature dependence for 6 K ≤ T ≤ 68 K. These rate constants are identical (Figure 2, open and filled circles) with the slow component extracted from the double-exponential fits to the relaxation transients of the combined Chl$_Z^+$–Q_A^- EPR signal, induced in CN^--treated Mn-depleted PSII preparations where the non-heme Fe(II) is diamagnetic. This is direct evidence that both sets of rate constants represent the intrinsic relaxation rates of Chl$_Z^+$. The absence of any contribution from an exchange interaction to the scalar rate constants is expected taking into account the 40 Å distance between the non-heme Fe(II) and the Chl$_Z^+$ radical. This distance is too long to allow for significant orbital overlap between the two species, as was also observed for $Y_D^•$ (Hirsh et al., 1992a) and for (BChla)$_2^+$ (Hirsh & Brudvig, 1993). These two radicals are at distances closer than 40 Å to the non-heme Fe(II) (~37 and 28 Å, respectively). A similar $T^{1.3}$ temperature dependence, indicative of a direct spin-phonon instead of a Raman relaxation process, has been observed for k_{1i} of (BChla)$_2^+$ in *Rb. sphaeroides* reaction centers over the temperature range 3.8 K ≤ T ≤ 22 K (Hirsh & Brudvig, 1993). Since the intrinsic relaxation rate constants of the (BChla)$^+$ and [Ni(II)-(OEP)$^{•/2}$]$_2$ models showed the usually observed quadratic temperature dependence, it was concluded that it is the especially rigid environment of (BChla)$_2^+$ which modulates its intrinsic relaxation and causes it to be different from the model systems. A review of the theory of the different spin–lattice relaxation processes (direct, Raman, and Orbach) has been presented in Scott and Jeffries (1962). It is mentioned that the direct process will have an appreciable contribution to the relaxation only at the lowest temperatures, since it is proportional to the number of phonons in a narrow band at the very low frequency end of the phonon spectrum. In the case of Chl$_Z^+$, the $\sim T^{1.0}$ temperature dependence of k_{1i} is seen in the entire range of temperatures examined (6 K ≤ T ≤ 68 K), which makes it a quite unusual behavior. The only explanation we can give at the present time is that the local environment of Chl$_Z$ in the PSII reaction center is (as in the case of the "special pair" in the reaction center from *Rb. sphaeroides*) highly rigid, so that for temperatures below 70 K only a narrow band of low-frequency lattice phonons is available for providing an efficient spin–lattice relaxation pathway. Our proposal that Chl$_Z^+$ is located at the periphery of the D1/D2 structural unit of PSII does not exclude the possibility of its environment maintaining its rigidity through a tight association with the cyt b_{559} protein.

Concluding Remarks. The combination of two different EPR spectroscopic methods has given valuable information on the location of Chl$_Z$ in PSII. Chl$_Z$ is shown not to be analogous to the "voyeur" monomer bacteriochlorophylls of the bacterial reaction center. Its proposed location on the hydrophobic surface of the D1/D2 complex could bring it in close association with cyt b_{559}. Thus, one could explain the fast reduction of Chl$_Z^+$ by cyt b_{559}; Chl$_Z^+$ is not observed as a kinetic intermediate in the photooxidation of cyt b_{559} (Buser et al., 1992). The possibility of Chl$_Z$ being associated with the process of photoinhibition is still plausible. It is possible that Chl$_Z^+$ quenches excitation energy via raditionless decay of the excited doublet to the ground state while cyt b_{559} remains oxidized. Further studies are needed to test this hypothesis and clarify the functional role of Chl$_Z^+$ in photosystem II.

ACKNOWLEDGMENT

We thank Dr. Harry Frank and Shariar Taremi of the University of Connecticut (Storrs) for providing the purified reaction centers of *Rb. sphaeroides* and Chris Coldren for helping with the computer graphic manipulations of the crystal structure of the reaction center from *Rps. viridis*. Special thanks to Xiao-Hui Jiang for preparing the Mn-depleted PSII membranes used in the pulsed EPR experiments, Dr. Donald Hirsh for his help with the experimental and theoretical aspects of this work, and Dr. Vasili Petrouleas for providing us with unpublished results on the CN^- treatment of PSII.

REFERENCES

Abragam, A. (1955) *Phys. Rev. 98*, 1729.

Abragam, A. (1961) *The Principles of Nuclear Magnetism*, Chapter 8, Clarendon Press, Oxford.

Beck, W. F., de Paula, J. C., Brudvig, G. W. (1985) *Biochemistry 24*, 3035.

Beck, W. F., Innes, J. B. & Brudvig, G. W. (1990) in *Current Research in Photosynthesis* (Baltscheffsky, M., Ed.) pp 817–820, Kluwer Academic, Dordrecht, The Netherlands.

Beck, W. F., Innes, J. B., Lynch, J. B., & Brudvig, G. W. (1991) *J. Magn. Reson. 91*, 12.

Beinert, H., & Orme-Johnson, W. H. (1967) In *Magnetic Resonance in Biological Systems* (Ehrenberg, A., Malmström, B. G., & Vänngård, T., Eds.) pp 221–247, Pergamon Press, Oxford.
Berthold, D. A.; Babcock, G. T., & Yocum, C. F. (1981) *FEBS Lett. 134*, 231.
Bloembergen, N. (1949) *Physica 15*, 386.
Buser, C. A. (1993) Ph.D. Thesis, Yale University.
Buser, C. A., Thompson, L. K., Diner, B. A., & Brudvig, G. W. (1990) *Biochemistry 29*, 8977.
Buser, C. A., Diner, B. A., & Brudvig, G. W. (1992) *Biochemistry 31*, 11449.
Castner, T. G. (1959) *Phys. Rev. 115*, 1506.
Deisenhofer, J., Epp, O., Miki, K., Huber, R., & Michel, H. (1984) *J. Mol. Biol. 180*, 385.
de Paula, J. C., Innes, J. B., & Brudvig, G. W. (1985) *Biochemistry 24*, 8114.
de Paula, J. C., Li, P. M., Miller, A.-F., Wu, B. W., & Brudvig, G. W. (1986) *Biochemistry 25*, 6487.
Evelo, R. G., & Hoff, A. J. (1991) *J. Magn. Reson. 95*, 495.
Goodman, G., & Leigh, J. S., Jr. (1985) *Biochemistry 24*, 2310.
Gounaris, K., Chapman, D. J., Booth, P., Crystall, B., Giorgi, L. B., Klug, D. R., Porter, G., & Barber, J. (1990) *FEBS Lett. 265*, 88.
Grant, J. L., Kramer, V. J., Ding, R., & Kispert, L. D. (1988) *J. Am. Chem. Soc. 110*, 2151.
Hirsh, D. J., & Brudvig, G. W. (1993) *J. Phys. Chem. 97*, 13216.
Hirsh, D. J., Beck, W. F., Innes, J. B., & Brudvig, G. W. (1992a) *Biochemistry 31*, 532.
Hirsh, D. J., Beck, W. F., Lynch, J. B., Que, L., Jr., & Brudvig, G. W. (1992b) *J. Am. Chem. Soc. 114*, 7475.
Hyde, J. S. (1979) in *Time-Domain Electron Spin Resonance* (Kevan, L., & Schwartz, R. N., Eds.) pp 1–30, John Wiley & Sons, New York.
Hyde, J. S., & Rao, K. V. S. (1978) *J. Magn. Reson. 29*, 509.
Innes, J. B., & Brudvig, G. W. (1989) *Biochemistry 28*, 1116.
Klimov, V. V., Allakhverdiev, S. I., Demeter, S., & Krasnovskii, A. A. (1980) *Dokl. Akad. Nauk SSSR 249*, 227.
Kobayashi, M., Maeda, H., Watanabe, T., Nakane, H., & Satoh, K. (1990) *FEBS Lett. 260*, 138.
Kolougliotis, D., Hirsh, D. J., & Brudvig, G. W. (1992) *J. Am. Chem. Soc. 114*, 8322.
Kulikov, A. V., & Likhtenstein, G. I. (1977) *Adv. Mol. Relax. Interact. Processes 10*, 47.
Michel, H., & Deisenhofer, J. (1988) *Biochemistry 27*, 1.
Montoya, G., Yruela, I., Picorel, R. (1991) *FEBS Lett. 283*, 255.
Nanba, O., & Satoh, K. (1987) *Proc. Natl. Acad. Sci. U.S.A. 84*, 109.
Nugent, J. H. A., Evans, M. C. W., & Diner, B. A. (1982) *Biochim. Biophys. Acta 682*, 106.
Nugent, J. H. A., Telfer, A., Demetriou, C., & Barber, L. (1989) *FEBS Lett. 255*, 53.
Okamura, M. Y., Feher, G., & Nelson, N. (1982) in *Photosynthesis: Energy Conversion by Plants and Bacteria* (Govindjee, Ed.) pp 195–272, Academic Press, New York.
Portis, A. M. (1953) *Phys. Rev. 91*, 1071.
Press, W. H., Flannery, B. P., Teukolsky, S. A., & Vetterling, W. T. (1989) *Numerical Recipes in Pascal*, Cambridge University Press, Cambridge.
Ruffle, S. V., Donnelly, D., Blundell, T. L., & Nugent, J. H. A. (1992) *Photosynth. Res. 34*, 287.
Sanakis, Y., Petrouleas, V., & Diner, B. A. (1994) *Biochemistry* (in press).
Schelvis, J. P. M., van Noort, P. I., Aartsma, T. J., & van Gorkom, H. J. (1994) *Biochim. Biophys. Acta 1184*, 242.
Scott, P. L., & Jeffries, C. D. (1962) *Phys. Rev. 127*, 32.
Thompson, L. K., & Brudvig, G. W. (1988) *Biochemistry 27*, 6653.
Visser, J. W. M., & Rijgersberg, C. P. (1975) in *Proceedings of the International Congress on Photosynthesis, 3rd* (Avron, M., Ed.) pp 323–334, Elsevier Biomedical, Amsterdam.
Visser, J. W. M., Rijgersberg, C. P., & Gast, P. (1977) *Biochim. Biophys. Acta 460*, 36.
Yeates, T. O., Komiya, H., Rees, D. C., Allen, J. P., & Feher, G. (1987) *Proc. Natl. Acad. Sci. U.S.A. 84*, 6438.
Yonetani, T., Yamamoto, H., Erman, J. E., Leigh, J. S., & Reed, G. H. (1972) *J. Biol. Chem. 247*, 2447.